Pictorial Essay | Neuroimaging and Head & Neck

http://dx.doi.org/10.3348/kjr.2016.17.5.664
pISSN 1229-6929 · eISSN 2005-8330
Korean J Radiol 2016;17(5):664-673

Korean Journal of Radiology
KJR

Eye Globe Abnormalities on MR and CT in Adults: An Anatomical Approach

James Thomas Patrick Decourcy Hallinan, MBChB, FRCR[1], Premilla Pillay, MD, FRCR[1], Lilian Hui Li Koh, MBBS, MMed (Ophth)[2], Kong Yong Goh, FRCOphth, FRCS (Edin), MMed (Ophth)[3, 4], Wai-Yung Yu, MBBS, FRCR[5]

[1]Department of Diagnostic Imaging, National University Health System, Singapore 119074; [2]National Healthcare Group Eye Institute, Tan Tock Seng Hospital, Level 1, TTSH Medical Centre, Singapore 308433; [3]Yong Loo Lin School of Medicine, National University of Singapore, Singapore 117597; [4]Dr. Goh Eye Neuro-Ophthalmic and Low Vision Specialist, Mount Elizabeth Novena Specialist Centre, Singapore 329563; [5]Department of Neuroradiology, National Neuroscience Institute, Singapore 308433

Eye globe abnormalities can be readily detected on dedicated and non-dedicated CT and MR studies. A primary understanding of the globe anatomy is key to characterising both traumatic and non-traumatic globe abnormalities. The globe consists of three primary layers: the sclera (outer), uvea (middle), and retina (inner layer). The various pathological processes involving these layers are highlighted using case examples with fundoscopic correlation where appropriate. In the emergent setting, trauma can result in hemorrhage, retinal/choroidal detachment and globe rupture. Neoplasms and inflammatory/infective processes predominantly occur in the vascular middle layer. The radiologist has an important role in primary diagnosis contributing to appropriate ophthalmology referral, thereby preventing devastating consequences such as vision loss.

Keywords: *Eye globe; CT; MRI; Trauma*

INTRODUCTION

Majority of eye globe imaging is performed secondary to CT and MRI imaging of the brain for various reasons ranging from trauma to neoplasia. Recent advances in MR and CT technology that allows for detailed visualisation of the globe has resulted in frequent, incidental detection of abnormalities.

Received August 23, 2015; accepted after revision June 5, 2016.
Corresponding author: James Thomas Patrick Decourcy Hallinan, MBChB, FRCR, Department of Diagnostic Imaging, National University Health System, 5 Lower Kent Ridge Rd, Singapore 119074.
• Tel: (65) 6779 5555 • Fax: (65) 6779 5678
• E-mail: jim.hallinan@gmail.com

Non-contrast CT is useful in the initial evaluation of orbital and globe trauma for the assessment of fractures, extra-ocular muscle herniation and suspected globe rupture. CT is the technique of choice for evaluating metallic or paramagnetic foreign bodies, whereas MRI is contraindicated due to potential migration and local heating. CT is also useful for evaluation of globe calcifications, especially in the case of retinoblastoma (1).

MRI provides exquisite soft tissue contrast and the sclera can be distinguished from the choroid and retina. Dedicated orbital MRI scans (1.5 or 3 tesla platforms) are performed in our institution using the following protocol; axial and coronal T1-weighted (T1W) with and without fat suppression, axial and coronal short tau inversion recovery (STIR) or fat suppressed T2-weighted (T2W) and multiplanar fat-suppressed gadolinium-enhanced T1W images. Table 1 shows the common MRI characteristics of the various structures in the globe. High-resolution MRI

Korean Journal of Radiology
KJR

facilitates evaluation of chorioretinal detachments and potential underlying neoplasms. The technique is limited by lengthy scanning time, increased cost compared to CT, and requirements for sedation in children and other non-compliant patient groups.

In order to interpret the globe abnormality, a primary understanding of the globe anatomy is necessary. The differential diagnosis can be made easier and refined by categorising the abnormalities according to the layers and the compartments of the globe. Knowledge of the imaging features of both traumatic and non-traumatic globe abnormalities is necessary to ensure appropriate ophthalmology referral and accurate diagnosis. In addition, knowledge of incidental degenerative changes, globe implants and fillers is important to prevent unnecessary work-up.

Globe Anatomy

The globe occupies one third of the orbital volume, with the vitreous humour representing two-thirds of the volume of the globe (2). The wall of the globe comprises three layers (Fig. 1), i.e., the fibrous coat (outer), uvea (middle), and retina (inner layer) enveloped by a fascial sheath known as Tenon's capsule (3).

Tenon's Capsule and Fibrous Coat (Outer Layer)

The outermost fibrous coat constitutes the sclera and cornea. The sclera is enveloped by the fibroelastic Tenon's capsule, which fuses with the bulbar conjunctiva and is perforated posteriorly by the optic nerve sheath. The episcleral space is a potential space that can extend between the fascia and the sclera (1).

The cornea is a key component of the refractive system and measures 0.5 mm in thickness centrally. On MRI, the cornea is a low signal intensity structure due to collagen but may be highlighted by an overlying slightly hyperintense tear film on T1W images. The sclera merges with the cornea at the limbus anteriorly. It is also composed of collagen, appearing hypointense on MRI and measuring up to 1 mm

Table 1. T1W and T2W Characteristics of Globe Structures

Layer	MRI Sequences-Normal Anatomical Features		Pathology by Region
	T1W	T2W	
Tenon's capsule	Not usually visible. Can be distended by fluid/hemorrhage accumulating in potential episcleral space		Effusions due to infection, inflammation, trauma (hemorrhage), neoplasms/metastases (Figs. 2, 3)
Cornea	Hypointense-can be highlighted by an overlying T1W hyperintense tear film	Hypointense	Traumatic, infective/inflammatory disruption (Figs. 4, 5)
Sclera	Hypointense	Hypointense	Episcleritis/scleritis: exudative chorioretinal detachment (Fig. 3) Staphylomas (Fig. 6) Colobomas Phthisis bulbi (Figs. 7, 8) Scleral bands (Figs. 8, 9) Scleral calcifications (Fig. 10)
Uveal tract, choroid	Hyperintense	Hypointense	Choroidal detachments (Figs. 11-13)
Retina	Hyperintense-not usually seen separately from underlying choroid	Hypointense	Retinal detachments (Fig. 11) Treated detachment, e.g., scleral bands (Figs. 8, 9), silicone oil (Fig. 14), and pneumatic retinopexy (Fig. 15) Ocular neoplasms: melanoma (Fig. 16), metastases (Fig. 17), vascular neoplasms/phakomatoses (Fig. 18) Uveitis (Fig. 19)
Aqueous/vitreous humour	Hypointense	Hyperintense	Endophthalmitis Posterior vitreous detachment
Lens	Hypointense	Hypointense	Lens prostheses Lens dislocation (Fig. 20)

T1W = T1-weighted, T2W = T2-weighted

in thickness. The sclera maintains intraocular pressure and is the insertion site for the extra-ocular muscles.

Uveal Tract (Middle Layer)

The uveal tract consists of the iris, ciliary body and choroid. The uveal tract is highly vascular and contains pigmented melanocytes. The iris is a pigmented circular structure responsible for controlling the size of the pupil. It attaches to the ciliary body, which consists of the aqueous humour producing anterior pars plicata and the posterior pars plana.

The ciliary body musculature attaches to the lens via the zonular fibers and is important for accommodation. The choroid merges with the ciliary body at the ora serrata and

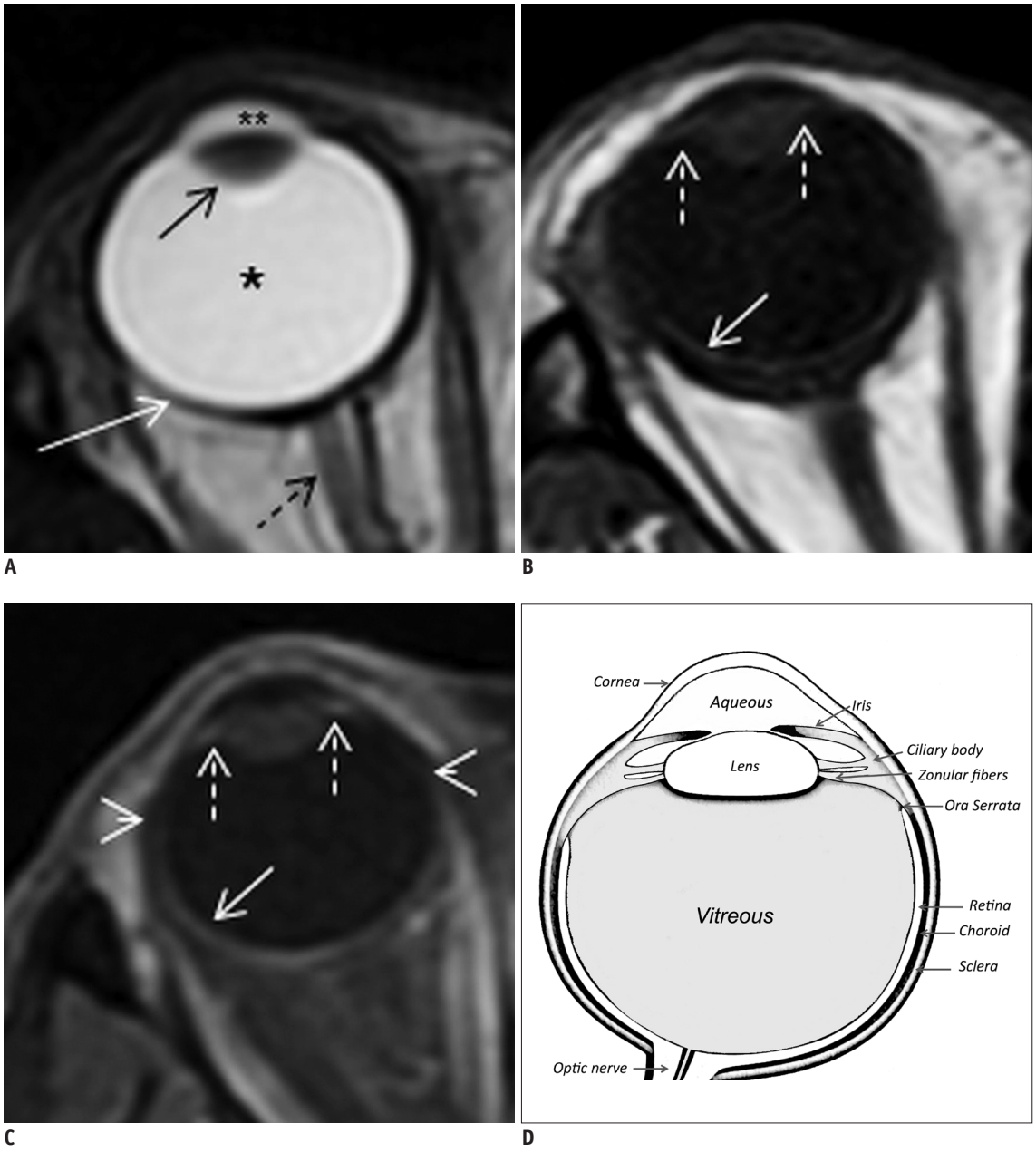

Fig. 1. Normal globe anatomy on orbital MRI.
Lens (black arrow) and sclera (white arrow) show hypointense signal on all sequences. **A.** On axial T2W images, vitreous (*) and aqueous humour in anterior chamber (**) are diffusely hyperintense. Optic nerve is labeled (dashed black arrow). **B.** Axial T1W image of right globe. Retina and choroid appear as single hyperintense layer (white arrow) with enhancement on fat-saturated post contrast T1W image (**C**, white arrow). Ciliary bodies form part of choroid (dashed white arrows, **B, C**). Approximate position of ora serrata is shown (small white arrowheads). **D.** Anotated illustration of globe for comparison with MRI anatomy. T1W = T1-weighted, T2W = T2-weighted

Korean Journal of Radiology
KJR

extends posteriorly to the optic nerve head. This structure provides nourishment to the retina (4). On MRI, the uveal tract appears hyperintense on T1W and hypointense on T2W images (Fig. 1).

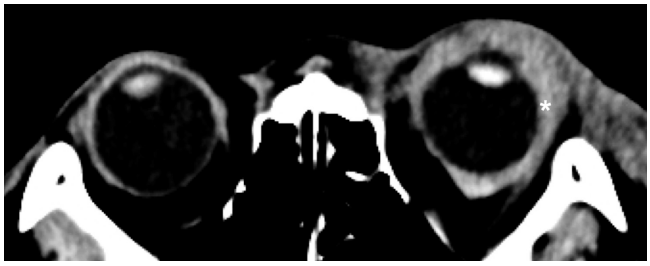

Fig. 2. Axial non-contrast image from post traumatic brain CT scan demonstrates expansion of left episcleral space by hyperdense hematoma (white asterisk), which extends posteriorly to surround globe likely within intra-conal space. Globe appears intact.

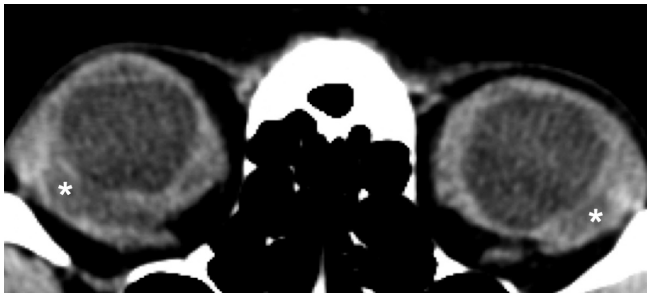

Fig. 3. Axial non-contrast enhanced image from orbital CT study on patient with history of Wegener's granulomatosis with posterior scleritis. Bilateral episcleral fluid collections (white asterisks) with distortion of globes are likely due to scleral degeneration or necrosis.

Retina (Inner Layer)

The retina is the innermost sensory layer of the globe and consists of two layers. The outer retinal pigment epithelium (RPE) is attached firmly to the choroid. The innermost sensory retina is responsible for visual perception. The layers are only tightly adherent at the optic disc and ora serrata where the RPE becomes continuous with the ciliary body. On MRI, the retina is in close apposition to the choroid in normal circumstances and cannot be discerned separately (1).

Vitreous Body

The vitreous body is a gel-like fluid bounded by the posterior and anterior hyaloid membranes. On MRI, the vitreous body appears hyperintense on T2W and hypointense

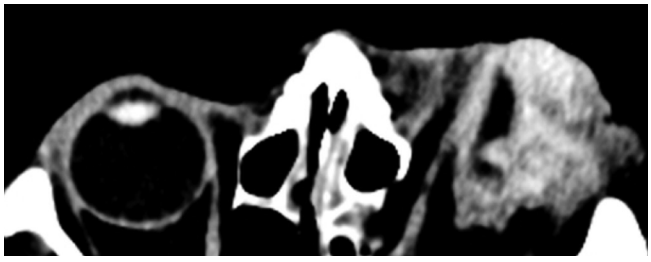

Fig. 4. Axial non-contrast image from brain CT for assessment of direct globe injury shows left globe rupture with complete loss of normal scleral contour, vitreous hemorrhage and surrounding periorbital and episcleral hematomas.

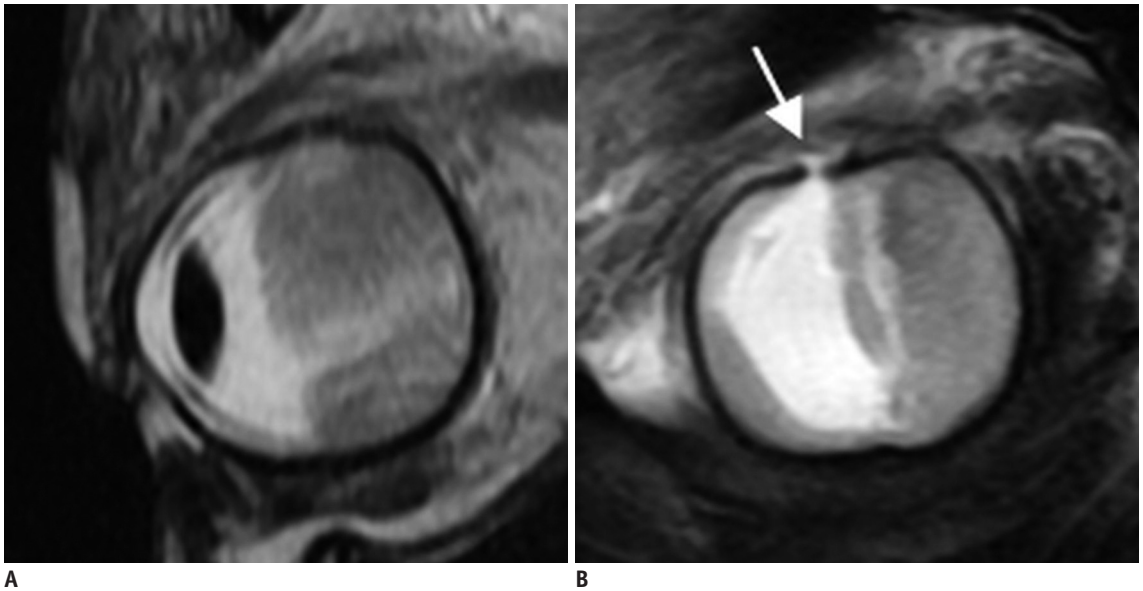

A **B**

Fig. 5. Sagittal T2W images (A, B) from orbital MRI study to detect post-traumatic globe rupture. Buckling and defect in superior sclera (**B**, white arrow) with loss of globe volume is consistent with globe rupture. Hypointense material in vitreous is suggestive of hemorrhage.
T2W = T2-weighted

on T1W images.

Lens

The lens forms the posterior boundary of the anterior chamber and is attached to the ciliary body via the zonular fibers. It is a transparent ovoid crystalline structure and MRI shows hypointensity on both T1W and T2W images.

Globe Pathology

Pathology of Tenon's Capsule/Episcleral Space

Effusions due to infection or inflammation of adjacent structures, traumatic hemorrhage and neoplasms including metastases can distend the episcleral space (Figs. 2, 3).

Fig. 6. Axial non-contrast image from orbital CT study for assessment of homonymous hemianopia. Bilateral focal protrusions through thinned sclera posteriorly are consistent with posterior staphylomas (white arrows).

Fig. 7. Axial non-contrast image from brain CT assessment of altered mental state shows right phthisis bulbi with irregular, scarred, shrunken right globe and dense internal calcification.

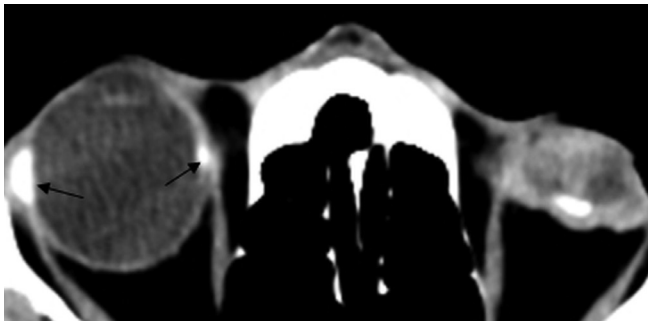

Fig. 8. Axial non-contrast image from brain CT assessment of traumatic head injury shows left phthisis bulbi with irregular, scarred, shrunken globe and left optic disc calcification. Scleral band for treatment of retinal detachment is seen on right (black arrows).

Pathology of the Sclera

Disruption of the sclera can result from trauma (globe rupture) (Figs. 4, 5) or secondary to degeneration, infection or inflammation. Episcleritis is typically a self-limiting

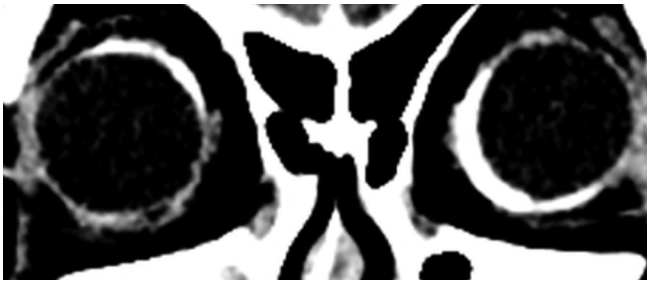

Fig. 9. Coronal non-contrast image from brain CT assessment of frequent falls. Bilateral bands of hyperdensity that do not conform to insertions of extra-ocular muscles, are consistent with prior bilateral scleral bands for treatment of retinal detachment. However, characteristic concavity at site of banding is not seen in this case.

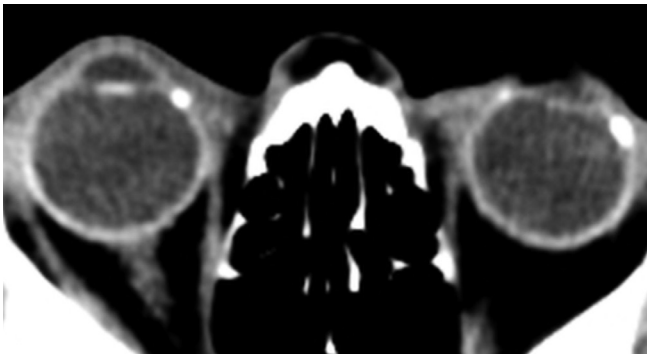

Fig. 10. Axial non-contrast image from brain CT assessment of altered mental state shows bilateral lens prostheses with incidental scleral calcifications at insertion of medial rectus on right and both medial and lateral recti on left. These calcifications represent normal part of aging. Scleral bands would appear more linear, as compared to punctate calcifications observed.

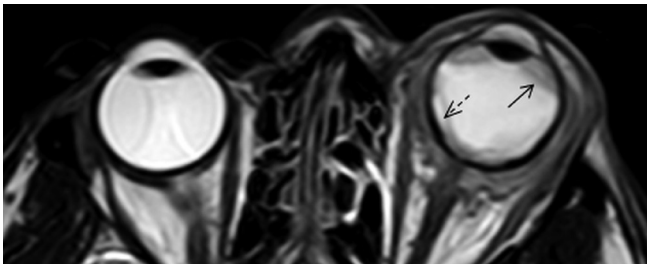

Fig. 11. Axial T2W image from orbital MRI study following direct left globe trauma shows iso- to hypointense episcleral material surrounding globe, consistent with hematoma. Choroidal (black arrow) and retinal (dashed black arrow) detachment is seen in left globe with underlying subchoroidal and subretinal fluid, respectively. T2W = T2-weighted

Korean Journal of Radiology
KJR

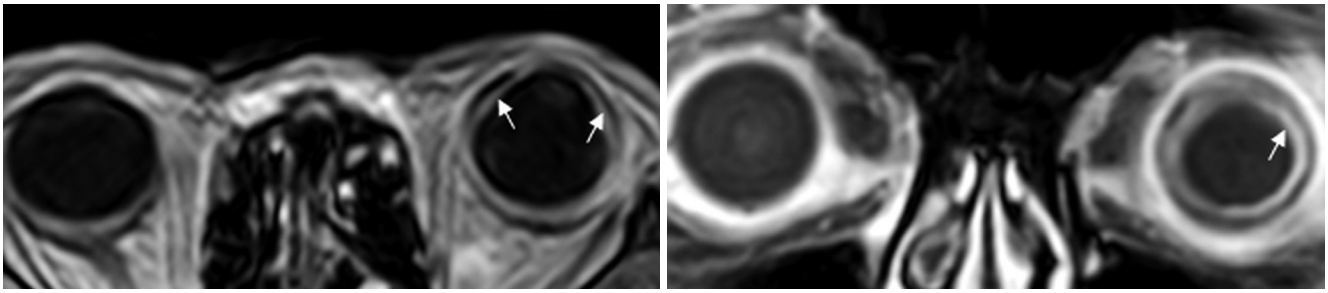

A B

Fig. 12. Axial T1W (A) and coronal T1W post gadolinium (B) images from orbital MRI study for suspected chorioretinal detachment and evaluation for any underlying lesion. Ciliochoroidal detachment extends anterior to expected location of ora serrata (**A**, white arrows). Enhancement of choroid is noted (**B**, white arrow), which is expected in detachment due to inflammatory response. Enhancing lesion suggestive of neoplastic cause is absent. T1W = T1-weighted

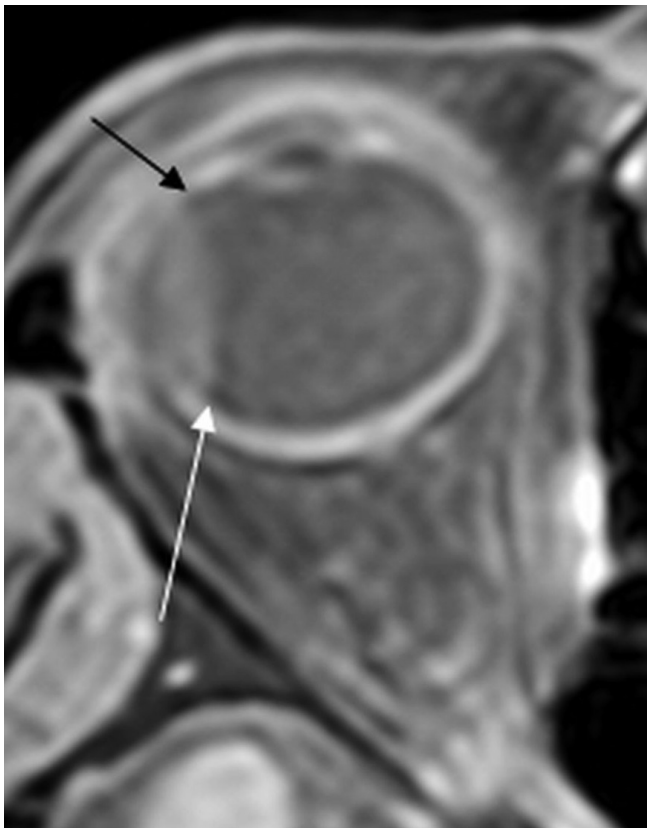

Fig. 13. Axial T1W post gadolinium image from orbital MRI study for right sided visual loss. Right choroidal detachment is seen limited posteriorly at expected location of vortex vein insertion (white arrow) and extending anterior to ora serrata (black arrow). Enhancement of detached choroid is also apparent as in Figure 12. Likewise, enhancing lesion suggestive of neoplastic cause is absent. T1W = T1-weighted

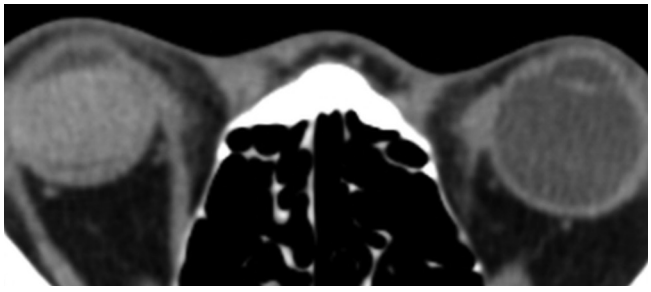

Fig. 14. Axial non-contrast image from brain CT assessment of altered mental state shows hyperdense material filling vitreous cavity on right with no evidence of overlying trauma or periorbital hematoma. This patient had undergone silicone oil injection for treatment of retinal detachment.

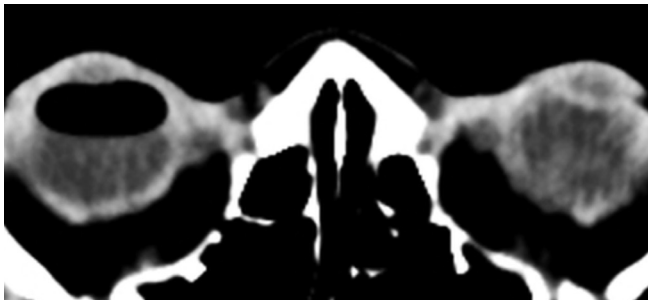

Fig. 15. Axial non-contrast image from brain CT assessment of altered mental state. Gas is noted in anterior vitreous compartment consistent with pneumatic retinopexy typically used in treatment of superior rhegmatogenous retinal detachments. No history of trauma was noted.

idiopathic disorder; whereas, scleritis is a more serious condition associated with connective tissue diseases such as rheumatoid arthritis. Scleritis may be complicated by exudative chorioretinal detachment and glaucoma (Fig. 3).

The sclera is altered in thickness and shape throughout life. Sustained intraocular pressure in childhood can lead to diffuse enlargement of the globe (buphthalmos); where as in adults, the more rigid sclera results in focal protrusions (staphylomas), especially in myopia (Fig. 6). Other globe shape abnormalities include colobomas (congenital defects in the layers of the globe including the optic disc) and phthisis bulbi representing an end-stage atrophic globe (Figs. 7, 8). Other scleral findings include scleral banding for treatment of retinal detachment (Figs. 8, 9) or incidental calcifications at the insertions of the recti in

elderly patients (Fig. 10) (1-3).

Pathology of the Uveal Tract and Retina

Retinal and Choroidal Detachment

Potential spaces for fluid accumulation and detachment can occur between the retinal layers due to the tenuous apposition (subretinal space), ciliary body/choroid and sclera (suprachoroidal space) and between the hyaloid base and retina (posterior hyaloid space) (2). The distinction between choroidal and retinal detachment is not always possible with MRI despite several known patterns. Anteriorly, choroidal detachments commonly extend into the ciliary body, whereas, retinal detachments are limited by the ora serrata. Posteriorly, choroidal detachments are limited by the insertions of the vortex veins; whereas, retinal detachments are limited by the optic disc producing a characteristic V shape (1).

Fundoscopy facilitates detection of retinal detachments, while contrast-enhanced MRI plays an essential role in the assessment of an underlying cause such as a neoplasm.

Choroidal detachments (Figs. 11-13) occur due to hemorrhage (trauma, prior surgical intervention or underlying neoplasm) or serous effusions (ocular hypotony or inflammation). Retinal detachments (Fig. 11) are commonly associated with a hole (rhegma) and are classified as rhegmatogenous or nonrhegmatogenous. Subretinal fluid accumulation can occur in nonrhegmatogenous detachments secondary to underlying neoplasms and hemorrhage. Gradual visual loss is the most common clinical finding. Rhegmatogenous detachments are commonly secondary to vitreous degeneration and traction on the retina.

Retinal detachments can be treated using scleral bands (Figs. 8, 9), pneumatic retinopexy, pars plana vitrectomy or injection of intraocular silicone oil (Figs. 14, 15) (5).

Ocular Neoplasms

Malignant melanoma represents the most common intraocular malignancy in adults and occurs in the pigmented uveal tract (3). Other globe neoplasms also predominantly involve the highly vascular uveal tract and include metastases (commonly breast and lung), benign neoplasms such as hemangiomas, and inflammatory processes such as sarcoidosis (6).

Malignant Melanoma

Malignant melanoma is most commonly unilateral and may present with pain or decreased visual acuity. Uveal

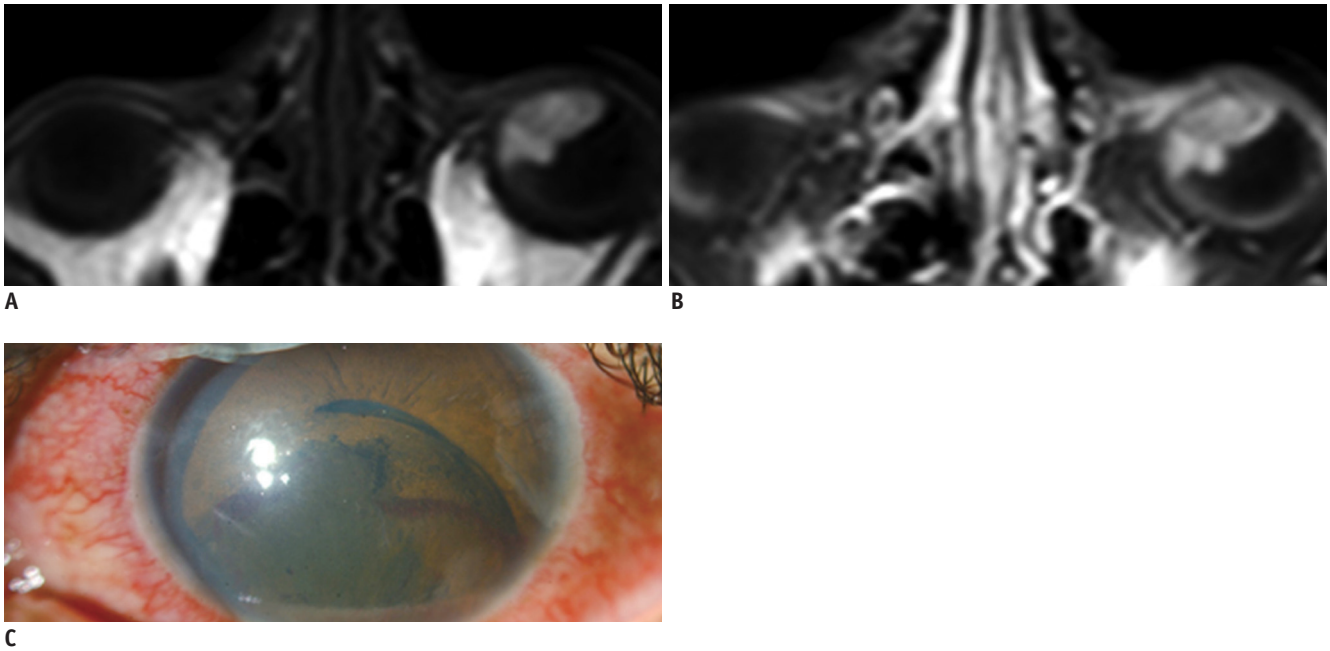

Fig. 16. Dedicated orbital MRI study for gradual left visual loss.
A. Axial T1WI shows lobulated hyperintense lesion arising in anteromedial left globe with endophytic extension into vitreous. **B.** T1WI post gadolinium shows enhancement of lesion with considerations including melanoma or hemorrhagic/mucinous metastasis. **C.** Corresponding photograph shows pigmented lesion arising from inferomedial globe wall with surrounding hemorrhage. Histology was consistent with uveal melanoma. T1W1 = T1-weighted image

Korean Journal of Radiology
KJR

melanomas are much less common than the cutaneous form. The appearance of melanoma is non-uniform on imaging due to the varying levels of melanin. On MRI, a typical melanoma is a focal mass at the periphery of the globe extending into the vitreous with propensity for retinal/choroidal detachment. Melanocytic tumors demonstrate hyperintensity on T1W images, intermediate/hypointense signal on T2W images and contrast enhancement (Fig. 16). Amelanotic tumors have a similar appearance to other neoplasms on MRI. In the presence of retinal detachments, it can be difficult to separate melanocytic melanoma from exudative/haemorrhagic retinal detachment, and contrast enhancement is a key discriminator. On CT, melanocytic melanomas appear slightly hyperdense and show contrast enhancement. MRI is the technique of choice for melanoma evaluation and assessment of episcleral extension that is an important prognostic feature occurring in approximately 13% of cases (7).

Ocular Metastases

The vascular uveal tract is the most common site for hematogenously disseminated metastases within the globe (Fig. 17). Breast and lung are the most common primary neoplasms leading to metastases. As with ocular melanoma, exophytic growth of the metastasis into the vitreous can result in retinal/choroidal detachment. T1W images are useful to distinguish metastases from melanocytic melanoma with the exception of hyperintense hemorrhagic or mucinous adenocarcinomas (6).

Vascular Neoplasms and Phakomatoses/Neurocutaneous Syndromes

Vascular neoplasms of the choroid are uncommon benign lesions usually seen in the second and third decades. Cavernous malformations may be associated with Sturge-Weber syndrome, and can be complicated by retinal tears and detachment. Capillary hemangiomas of the retina occur

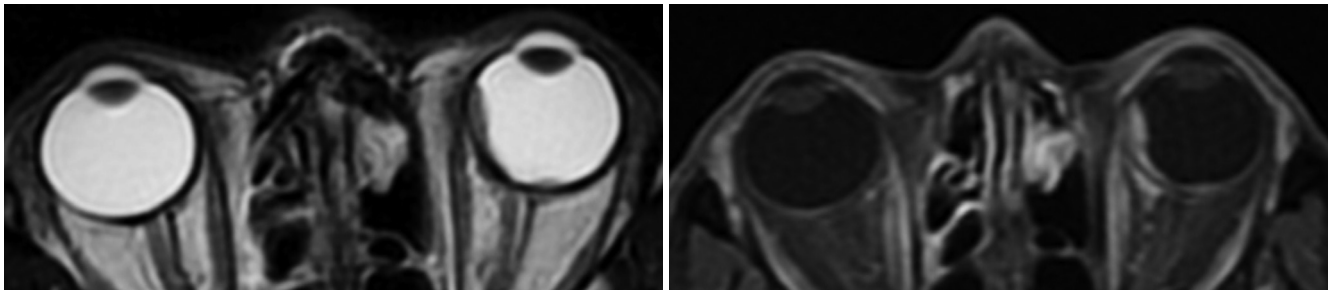

A B

Fig. 17. Male primary lung adenocarcinoma patient presenting with left sided blindness.
Axial T2W **(A)** and axial T1W **(B)** post gadolinium images from orbital MRI study show T2W hypointense intraocular lesions arising adjacent to sclera in left medial globe and close to left optic nerve head. Medial lesion shows contrast enhancement. Considerations include metastases (highly likely given clinical history) with amelanocytic melanoma (no T1W hypointensity; images not shown), less likely differential. No choroidal detachment is detected. T1W = T1-weighted, T2W = T2-weighted

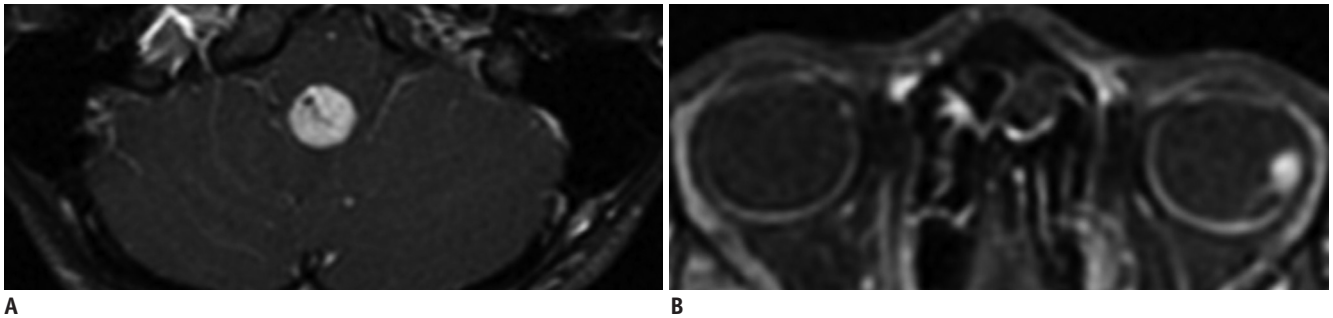

A B

Fig. 18. Axial T1W post gadolinium images of posterior fossa (A) and orbits (B) from brain and orbital MRI on patient who presented with headaches.
Enhancing lesion is observed in region of fourth ventricle complicated by hydrocephalus (not shown). Additional avidly enhancing lesion is seen arising from lateral choroid of left globe without associated chorioretinal detachment. These findings are suggestive of cerebellar and retinal/choroidal hemangioblastomas, although associated cystic component for cerebellar lesion is more typical. Underlying Von Hippel-Lindau disease was key consideration. Metastases are less likely given patient's young age (< 40 years old) and no known history of primary malignancy. Histology following resection of cerebellar lesion confirmed diagnosis of hemangioblastoma. T1W = T1-weighted

in a quarter to half of patients with Von Hippel-Lindau syndrome and are histologically similar to the associated cerebellar hemangioblastoma (Fig. 18). These lesions are supplied by dilated feeder vessels with propensity for retinal hemorrhage and detachment. They are often small, but can sometimes be visualised on MRI as hyperintense on T1W images, and hyperintense on T2W images (8).

Uveitis

Inflammation of the uveal tract commonly involves the adjacent retina and sclera (Fig. 19). Uveitis can be serious possibly leading to permanent visual loss. It is often idiopathic in nature, although numerous infective and inflammatory causes are described including connective tissue diseases such as sarcoidosis and toxoplasmosis. CT or MR evaluation may be useful in posterior uveitis, for assessment of complications including chorioretinal detachment, underlying abscesses or foreign bodies providing a nidus for infection (9).

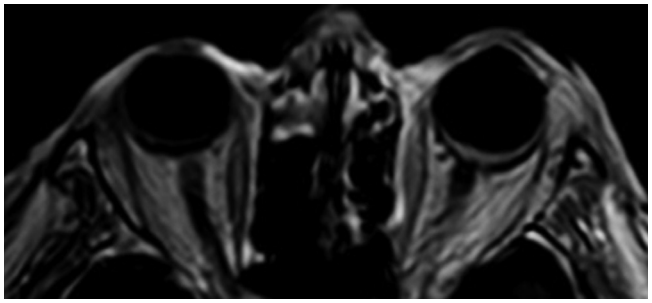

Fig. 19. Axial T1WI post gadolinium image from orbital MRI study performed for globe pain and acute visual loss. Thickening and enhancement of left retina, posterior choroid and optic disc are observed, suggestive of posterior uveitis, which may be associated with inflammatory conditions such as sarcoidosis or infections such as toxoplasma or cytomegalovirus. Underlying neoplasm, e.g., metastasis was less likely as no focal lesion was detected. Patient was not available for follow-up. T1W1 = T1-weighted image

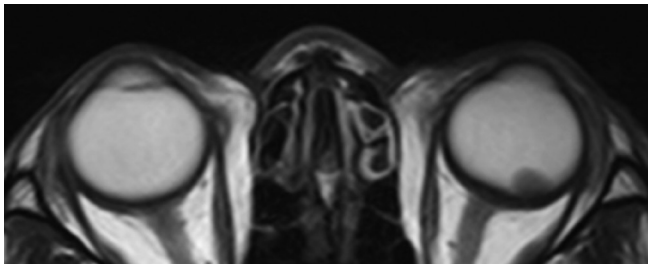

Fig. 20. Axial T2W image from orbital MRI study for evaluation of left visual loss shows left sided lens dislocation (lens luxation) with hypointense lens lying dependently adjacent to retina in posterior vitreous humour. No history of trauma or prior ocular inflammation was noted. Right-sided lens prosthesis is noted. T2W = T2-weighted

Pathology of the Lens, Anterior and Posterior Chambers

Lens Prostheses

Lens prostheses are readily identifiable on CT and MRI. Lens dislocation can be well visualised and is typically secondary to trauma or degeneration of the zonular fibers (Fig. 20) (10).

Endophthalmitis

Endophthalmitis represents inflammation or infection involving the anterior chamber and vitreous humour. Despite aggressive therapy, the outcome remains poor resulting in pthisis bulbi and visual loss. The most common organisms include skin commensals such as staphylococcus epidermis, candida and parasites including cysticercosis and toxocariasis. CT and MRI may demonstrate uveal thickening and enhancement, chrorioretinal or vitreous detachment and increased density or T1W hyperintensity of the vitreous due to proteinaceous exudates (2). Diffusion-weighted imaging can also be useful for diagnosis of endophthalmitis and typically demonstrates hyperintensity and corresponding reduced apparent diffusion coefficient values in the anterior chamber and/or vitreous (11).

Posterior Vitreous Detachment

In old age, the vitreous may shrink and form clumps leading to 'floaters'. This process of shrinkage may result in traction causing separation of the posterior hyaloid membrane from the sensory retina termed posterior vitreous detachment. Accelerated vitreous degeneration may result from trauma, inflammation (endophthalmitis) or significant myopia (1). On MR and CT, posterior vitreous detachment appears as a membrane within the vitreous cavity detached from the optic disc and attached at the ora serrata. Fluid may also accumulate in the retrohyaloid space.

CONCLUSION

A multitude of globe abnormalities can be detected and characterised on CT and MRI studies. Understanding the anatomy is a key component in the structured approach to a differential diagnosis. An understanding of the CT attenuation and MRI signal characteristics can also help in characterising the lesions, especially in the case of uveal melanoma. The radiologist has an important role in the primary diagnosis of clinically significant and potentially treatable globe abnormalities contributing to rapid referral

Korean Journal of Radiology
KJR

and improved outcomes.

REFERENCES

1. Roy AA, Davagnanam I, Evanson J. Abnormalities of the globe. *Clin Radiol* 2012;67:1011-1022
2. Van Tassel P, Mafee MF, Atlas SW, Galetta SL. *Chapter 23. Eye, orbit and visual system*. In: Atlas SW, ed. *Magnetic resonance imaging of the brain and spine*, Volume 2, 4th ed. Philadelphia: Lippincott Williams & Wilkins, 2009:1258-1363
3. Mafee MF, Karimi A, Shah J, Rapoport M, Ansari SA. Anatomy and pathology of the eye: role of MR imaging and CT. *Neuroimaging Clin N Am* 2005;15:23-47
4. Goh PS, Gi MT, Charlton A, Tan C, Gangadhara Sundar JK, Amrith S. Review of orbital imaging. *Eur J Radiol* 2008;66:387-395
5. Lane JI, Watson RE Jr, Witte RJ, McCannel CA. Retinal detachment: imaging of surgical treatments and complications. *Radiographics* 2003;23:983-994
6. Ahmad SM, Esmaeli B. Metastatic tumors of the orbit and ocular adnexa. *Curr Opin Ophthalmol* 2007;18:405-413
7. Laver NV, McLaughlin ME, Duker JS. Ocular melanoma. *Arch Pathol Lab Med* 2010;134:1778-1784
8. Smoker WR, Gentry LR, Yee NK, Reede DL, Nerad JA. Vascular lesions of the orbit: more than meets the eye. *Radiographics* 2008;28:185-204; quiz 325
9. LeBedis CA, Sakai O. Nontraumatic orbital conditions: diagnosis with CT and MR imaging in the emergent setting. *Radiographics* 2008;28:1741-1753
10. Kubal WS. Imaging of orbital trauma. *Radiographics* 2008;28:1729-1739
11. Rumboldt Z, Moses C, Wieczerzynski U, Saini R. Diffusion-weighted imaging, apparent diffusion coefficients, and fluid-attenuated inversion recovery MR imaging in endophthalmitis. *AJNR Am J Neuroradiol* 2005;26:1869-1872